Iterative Source-Channel Decoding for Error-Resilient Image Transmission Using a Markov Random Field Source Model

Jörg Kliewer [1], Norbert Görtz [2], and Alfred Mertins [3]

[1] University of Kiel, Institute for Circuits and Systems Theory (LNS)
24143 Kiel, Germany, jkl@tf.uni-kiel.de

[2] Munich University of Technology (TUM), Institute for Communications Engineering (LNT)
80290 Munich, Germany, norbert.goertz@ei.tum.de

[3] University of Oldenburg, Signal Processing Group
26111 Oldenburg, Germany, alfred.mertins@uni-oldenburg.de

Abstract

In this paper, we propose a joint source-channel decoding approach for the robust image transmission over wireless channels. In addition to the explicit redundancy coming from channel codes, we also use implicit residual source redundancy for error protection. The source redundancy is modeled by a Markov random field (MRF) source model, which considers the residual spatial correlation after source encoding. Due to the link between MRFs and the Gibbs distribution, the source decoder can be implemented with low complexity. At the decoder we use an iterative source-channel decoder which can be obtained in the same manner as for serially concatenated channel codes. As a novel result we show that this iterative decoding scheme in combination with a simplified joint allocation of source and channel coding rates can be successfully employed for recovering the image data, especially when the channel is highly corrupted.

1 Introduction

Recently, joint source-channel coding approaches have become a reasonable alternative compared to the strict application of Shannon's source-channel separation principle especially for delay- or complexity-constrained systems. One subclass of those approaches is represented by a joint allocation of source and channel coding rates such that the reconstruction error at the decoder is minimized. Often these techniques are used in combination with a state-of-the-art source coder and an elaborate error protection scheme for the highly sensitive source-encoded bitstream (e.g. [1], [2]). These methods provide excellent results for moderately distorted channels, however, especially for low channel signal-to-noise ratios (SNRs) their performance highly depends on the properties of the used channel codes.

Another subclass of joint source-channel coding is given by joint source-channel *de*coding, where residual source redundancy is exploited for additional error protection at the decoder. Some approaches even do not use channel codes at all and design the source encoder such that the residual index-based redundancy in the resulting bitstream alone is sufficient to provide reasonable error protection at the decoder (e.g. [3], [4]). These methods have less encoding delay and complexity, and for very low channel SNRs, they often yield similar or better performance than the combination of strong source and channel encoding.

In this paper, we combine the ideas from both subclasses mentioned above and present an iterative joint source-channel decoding approach for robust image transmission, where *both* the implicit residual index correlation after source-encoding and the explicit redundancies from channel codes are used for protecting the data. Furthermore, in the encoder of the proposed image transmission system the source and channel encoding rates are jointly allocated in a rate-distortion sense. As a new result the two-dimensional residual spatial correlation of the source image is modeled via a Markov random field (MRF) approach [5], [6], which has the advantage that it is not necessary to store *a priori* information describing the residual source correlation at the decoder. This is in contrast to those approaches which model the image data as Gauss-Markov processes, as for example the methods proposed in [4], [7]. The proposed technique utilizes an iterative source-channel decoding scheme [8] analog to the decoding of serially concatenated channel codes [9], where the outer constituent soft-input/soft-output (SISO) channel decoder is replaced by the MRF-based SISO source decoder.

2 Description of the Transmission System

The block diagram of the overall transmission system is depicted in Fig. 1. The two-dimensional (2-D) subband

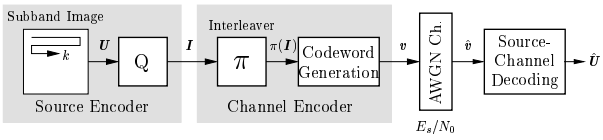

Fig. 1. Model of the transmission system

image is scanned in order to obtain the one-dimensional (1-D) subband vector $\boldsymbol{U}=[U_0,U_1,\ldots,U_{N-1}]$ consisting of N source values U_k. After subsequent (vector-) quantization, the resulting indices $I_k \in \mathcal{I}$ are represented with M bits, and thus can be described with the finite alphabet $\mathcal{I}=\{0,1,\ldots,2^M-1\}$. We can generally assume that there are dependencies between the elements of the index vector $\boldsymbol{I}=[I_0,I_1,\ldots,I_{N-1}]$ due to delay and complexity constraints for the source encoder.

In the channel encoder the bitstream is first interleaved in order to provide uncorrelated bits for the following codeword generation step using a rate-R_C systematic channel code. We obtain the code bit vector $\boldsymbol{v}=[\pi(\boldsymbol{I}),\boldsymbol{c}]$ where $\boldsymbol{v}=[v_0,v_1,\ldots,v_{N_v-1}]$ with $v_k \in \{0,1\}$, $N_v = N\cdot M/R_C$, and $\boldsymbol{c}$ referring to the redundancy bits. The code bit vector $\boldsymbol{v}$ is then transmitted over an AWGN channel, where coherently detected BPSK is used for the modulation. The conditional p.d.f. for the received soft bit $\hat{v}_m \in \mathbb{R}$ at the channel output given the transmitted bit v_m, $m=0,1,\ldots,N_v-1$, can be written as

$$p(\hat{v}_m \mid v_m) = \frac{1}{\sqrt{2\pi}\sigma_e}\, e^{-\frac{1}{2\sigma_e^2}\left(\hat{v}_m - v'_m\right)^2}, \quad v'_m = 1-2\,v_m, \tag{1}$$

and $\sigma_e^2 = \frac{N_0}{2E_s}$ denoting the channel noise variance. E_s is the energy to transmit each bit and N_0 corresponds to the one-sided power spectral density of the noise. Using conditional log-likelihood ratios (L-values) we may express (1) also as

$$L(\hat{v}_m \mid v_m) = \ln\left(\frac{p(\hat{v}_m \mid v_m=0)}{p(\hat{v}_m \mid v_m=1)}\right) = 4\,\frac{E_s}{N_0}\,\hat{v}_m = L_c\,\hat{v}_m. \tag{2}$$

The source-channel decoding step in Fig. 1 then provides an estimate of the input vector $\boldsymbol{U}$ in such a way that the SNR at the decoder output is maximized.

3 Joint Allocation of Source and Channel Coding Rates

When considering the transmission model in Fig. 1 for every subband in a subband image compression scheme, we have the additional problem of choosing the individual bit rates for the subbands and the channel coding rates for a given rate budget R_T such that the resulting distortion in the reconstructed signal is minimized. In the following, we propose a suboptimal strategy for jointly assigning the source and channel coding rates $\mathbf{r}_S = [R_S^{(0)},\ldots,R_S^{(j)},\ldots,R_S^{(K-1)}]$ and $\mathbf{r}_C = [R_C^{(0)},\ldots,R_C^{(j)},\ldots,R_C^{(K-1)}]$, with $R_{S/C}^{(j)}$ denoting the corresponding rates in the j-th subband and K representing the overall number of subbands. For simplicity reasons we restrict ourselves to the case where the only method of error protection is channel coding (i.e., we use source decoding by table lookups). The proposed method is based on the rate-distortion-optimal bit allocation algorithm from [10], which is modified such that also the error correction capabilities of the channel codes and the additional channel noise is incorporated in the distortion measure.

In order to obtain a transmission with bit error rate (BER) p_e over an AWGN channel we know from Shannon's channel coding theorem that under idealized conditions [11]

$$H(\boldsymbol{I})\,R_C\,f(p_e)/M \;\le\; C_{\text{AWGN}}(E_s/N_0) \tag{3}$$
$$\text{with } f(p_e) := 1 + p_e\log_2(p_e) + (1-p_e)\log_2(1-p_e)$$

has to be satisfied. Herein, $H(\boldsymbol{I})$ denotes the entropy of the source index vector $\boldsymbol{I}$, and $C_{\text{AWGN}}(\cdot)$ is the capacity of the binary-input AWGN channel, which depends on the parameter E_s/N_0. By using the equality in (3) and applying it to every subband j we obtain a relation between the actual BER $p_e^{(j)}$ on the one hand, and the channel coding rate $R_C^{(j)}$, the quantized source signal $Q[\boldsymbol{U}^{(j)},R_S^{(j)}]$ with rate $R_S^{(j)}$, and the channel capacity on the other hand:

$$f(p_e^{(j)}) = \frac{C_{\text{AWGN}}(E_s/N_0)\cdot M^{(j)}}{R_C^{(j)}\cdot H(Q[\boldsymbol{U}^{(j)},R_S^{(j)}])} \tag{4}$$

for $j=0,\ldots,K-1$. $M^{(j)}$ refers to the word length in the j-th subband and depends on the actual rate $R_S^{(j)}$. A worst case estimate for the distortion $D(p_e^{(j)},R_S^{(j)},R_C^{(j)})$ in the j-th subband after decoding can be now achieved in the following way: Let $P_\nu^{(j)}$, $\nu=0,1,\ldots,M^{(j)}$, denote the probability that ν bits are received wrongly when the $M^{(j)}$-bit codeword $I_k^{(j)}=\lambda$ is transmitted over a binary symmetric channel with error probability $p_e^{(j)}$. Then, $P_\nu^{(j)}$ can be specified as

$$P_\nu^{(j)} = \binom{M^{(j)}}{\nu}\left(p_e^{(j)}\right)^\nu\left(1-p_e^{(j)}\right)^{M^{(j)}-\nu} \tag{5}$$

where $p_e^{(j)}$ is derived by solving (4). A reconstructed distorted subband value $\bar{U}_k^{(j)}$ at time instant k can now be generated within the encoder as

$$\bar{U}_k^{(j)} = P_0^{(j)}\cdot U_q(\lambda,R_S^{(j)}) + \sum_{\nu=1}^{M^{(j)}} P_\nu^{(j)}\cdot U_q(\bar{\lambda}(\nu),R_S^{(j)}),$$
$$\text{with}\quad \bar{\lambda}(\nu) = [\bar{\lambda}_0,\ldots,\bar{\lambda}_{\nu-1},\bar{\lambda}_\nu,\ldots,\lambda_{M^{(j)}-1}]$$
$$\text{and}\quad \bar{\lambda}_\ell = 1-\lambda_\ell \tag{6}$$

for $\ell=0,1,\ldots,\nu-1$. $U_q(\lambda,R_S^{(j)})$ refers to the λ-th entry of the quantization table, which leads to a

source coding rate $R_S^{(j)}$, and $\lambda_\ell \in \{0,1\}$ denotes a single bit of the index λ. The distorted value $\bar{U}_k^{(j)}$ can thus be obtained by successive flipping of bits in the binary representation of the index λ starting with the most significant bit. The corresponding entries of the quantization table are then weighted with the probabilities $P_\nu^{(j)}$ from (5). Finally, the distortion $D(p_e^{(j)}, R_S^{(j)}, R_C^{(j)})$ can be calculated from the mean squared error between $\bar{U}_k^{(j)}$ and the undistorted source value $U_k^{(j)}$.

The rate allocation scheme can now be summarized as follows:

1. Calculate $D(p_e^{(j)}, R_S^{(j)}, R_C^{(j)})$, $j = 0, 1, \ldots, K-1$, by using (4), (5), and (6) for all combinations of $R_S^{(j)}$, $R_C^{(j)}$, and the given E_b/N_0 on the channel. Here, $E_b = E_s/R_{C,\text{overall}}$, where $R_{C,\text{overall}}$ denotes the channel coding rate for the *whole* image.
2. Obtain an optimal allocation for $\mathbf{r}_S$ and $\mathbf{r}_C$, given the rates and distortions from step 1 and the overall rate budget R_T, by using a modification of the bit-allocation algorithm from [10], where also the channel coding rates are included in the optimization.
3. In order to allow for equal transmission energy for all bits in the whole image, update $R_{C,\text{overall}}$ by using $\mathbf{r}_C$ from step 2. Go to step 1 and iterate until there is no further improvement for the vectors $\mathbf{r}_C$ and $\mathbf{r}_S$.

4 MRF-based SISO Source Decoding

In this section only the residual source redundancy after source encoding is exploited for error protection, i.e. no channel codes are used. Thus, in the transmission system from Fig. 1 we therefore have $\boldsymbol{v} = \boldsymbol{I}$.

In the following we derive a SISO source decoder based on a MRF source model which generates *a posteriori* probabilities (APPs) for the source hypotheses $I_k = \lambda$. To this end, let us consider the eight nearest neighbors for a given subband source index I_k within a quantized subband image *prior* to transmission. Such a neighborhood system is displayed in Fig. 2(a), where all neighboring source indices are referenced relatively to the index $I_{k,0,0}$ under consideration, which for the sake of brevity will also simply be written as I_k in all future discussions. We denote the set of all source indices belonging to the neighborhood of I_k as $\mathcal{N}_{I_k} = \{I_{k,q,j} \colon \ q,j = -1,0,1\} \backslash I_k$ in the following. Since all indices in the neighborhood system of Fig. 2(a) show spatial dependencies due to imperfect source encoding the index probabilities $P(I_k = \lambda)$, $\lambda \in \mathcal{I}$, may be modeled via a MRF using the well-known Markov-Gibbs correspondence [5]. Using this relation, the probability for an element I_k of the MRF given all other source indices in a local neighborhood $\mathcal{N}_{I_k}$ can then be stated as [5]

$$P(I_k = \lambda \,|\, \mathcal{N}_{I_k}) = \frac{1}{Z}\, e^{-\frac{1}{T} U(\lambda, \mathcal{N}_{I_k})}, \tag{7}$$

where the function $U(\lambda, \mathcal{N}_{I_k})$ is called energy function, the quantity T is called temperature, and Z denotes a normalization constant. We can decompose $U(\lambda, \mathcal{N}_{I_k})$ as a sum over so-called potential functions $V_C(\lambda, \mathcal{N}_{I_k})$ according to

$$U(\lambda, \mathcal{N}_{I_k}) = \sum_C V_C(\lambda, \mathcal{N}_{I_k}). \tag{8}$$

The potential functions are defined for a given clique C, and the sum in (8) is carried out over all or a subset of all possible cliques in the local neighborhood. An example is depicted in Fig. 2(b) for the eight-pixel neighborhood system in Fig. 2(a) where all associated cliques are shown. The first type of clique just consists of single source indices, the second type of cliques describes the index I_k and its horizontal neighbors, the third type addresses all vertical neighbors of I_k and so on. In the following we restrict ourselves only to

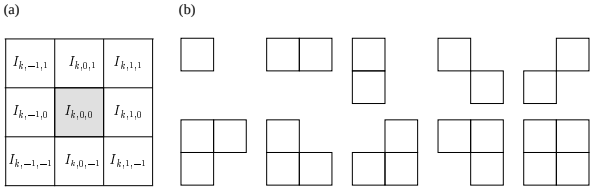

Fig. 2. Eight-pixel neighborhood system with all ten corresponding cliques

two-element cliques and the potential functions

$$V_C(\lambda, I_{k,q,j}) = |\lambda - I_{k,q,j}|^\delta \tag{9}$$

proposed in [12], where δ is a free parameter.

In order to apply the MRF model to the source decoder we consider a new set $\mathcal{N}_{\tilde{I}_k} = \{\tilde{I}_{k,q,j} \colon \ q,j = -1,0,1\} \backslash \tilde{I}_k$ where $\tilde{I}_{k,q,j}$ now denotes an *already decoded* estimate of $I_{k,q,j}$, e.g. from a maximum-likelihood (ML) decoding of the received soft-bits at the channel output. The APPs for $I_k = \lambda$ based on the local neighborhood at the decoder can then be written as $P(I_k = \lambda \,|\, \hat{I}_k, \mathcal{N}_{\tilde{I}_k})$, where the soft-bit vector $\hat{I}_k = [\hat{i}_{0,k}, \hat{i}_{1,k}, \ldots, \hat{i}_{M-1,k}]$ consists of the individual soft-bits $\hat{i}_{\ell,k} \in \mathbb{R}$ received at the output of the channel. By applying the Bayes theorem we obtain

$$P(I_k = \lambda \,|\, \hat{I}_k, \mathcal{N}_{\tilde{I}_k}) = C_k \cdot p(\hat{I}_k \,|\, I_k = \lambda) \cdot P(I_k = \lambda \,|\, \mathcal{N}_{\tilde{I}_k}) \tag{10}$$

with the normalization constant C_k. In (10) the term $p(\hat{I}_k \,|\, I_k = \lambda)$ denotes soft-information from the output of the AWGN channel according to

$$p(\hat{I}_k \,|\, I_k = \lambda) = \prod_{\ell=0}^{M-1} p(\hat{i}_{\ell,k} \,|\, i_{\ell,k}) \tag{11}$$

where the conditional p.d.f. $p(\hat{i}_{\ell,k} \,|\, i_{\ell,k})$ for the ℓ-th bit $i_{\ell,k}$ of the index I_k is given in (1) when v_m is replaced with $i_{\ell,k}$. The term $P(I_k = \lambda \,|\, \mathcal{N}_{\tilde{I}_k})$ corresponds to the conditional probability from (7) where the original source indices $I_{k,q,j}$, for the neighborhood are replaced by the estimates $\tilde{I}_{k,q,j}$.

Like in classical Bayesian MRF-based image restoration [5] we use an iterative decoding approach where (10) is applied multiple times until convergence is achieved. The procedure is as follows:

1. Obtain initial estimates $\tilde{I}_k^{(0)}$ for the received 1-D scanned subband image indices by performing a ML decoding from the received soft-bit sequence $\hat{\boldsymbol{I}}$ at the channel output. Set $r \leftarrow 0$.
2. Apply (10) in order to determine the APPs $P(I_k = \lambda \,|\, \hat{I}_k, \mathcal{N}_{\tilde{I}_k^{(r)}})$.
3. Obtain a new estimate $\tilde{I}_k^{(r+1)}$ via a maximum *a posteriori* (MAP) estimation according to
$$\tilde{I}_k^{(r+1)} = \arg \max_{\lambda} P(I_k = \lambda \,|\, \hat{I}_k, \mathcal{N}_{\tilde{I}_k^{(r)}}).$$
4. Set $r \leftarrow r+1$ and go to step 2 as long as the estimates $\tilde{I}_k^{(r)}$ change between iterations.

The resulting APPs $P(I_k = \lambda \,|\, \hat{I}_k, \mathcal{N}_{\tilde{I}_k^{(r)}})$ at the output of the last iteration may be interpreted as approximations of the APPs $P(I_k = \lambda \,|\, \hat{I}_k, \mathcal{N}_{\hat{I}_k})$ conditioned on all received soft-bit vectors $\hat{I}_{k,q,j}$ in the local neighborhood of $\hat{I}_k$.

The calculated APPs can then be used for a mean-squares estimation of the reconstructed source value $\hat{U}_k$, which corresponds to the demand for maximal reconstruction SNR, according to

$$\hat{U}_k = \sum_{\lambda=0}^{2^M-1} U_q(\lambda, R_S) \cdot P(I_k = \lambda \,|\, \hat{I}_k, \mathcal{N}_{\hat{I}_k}). \qquad (12)$$

5 Iterative Source-Channel Decoding

An error protection carried out by only using the residual spatial source redundancy may not be enough in many transmission situations. Therefore, we assume that the output of the source encoder is protected by a systematic channel code, as it is depicted in Fig. 1. Note that this scheme is highly similar to a serially concatenated channel code. Therefore, we can apply an iterative decoding scheme, where the outer constituent channel decoder is replaced by the MRF-based source decoder presented in Section 4.

The structure of the resulting decoder is depicted in Fig. 3. At the beginning of the first iteration, the SISO channel decoder issues APPs $P(i'_{\ell,k} \,|\, \hat{\boldsymbol{v}})$ for the information bits $i'_{\ell,k}$ of the bit-interleaved source index sequence $\pi(\boldsymbol{I})$. These APPs are

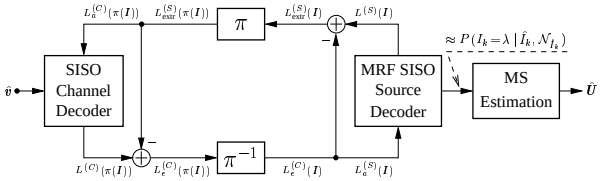

Fig. 3. Structure of the iterative source-channel decoder

used to calculate the corresponding conditional L-values $L^{(C)}(i'_{\ell,k}) = L_c\,\hat{i}'_{\ell,k} + L_a^{(C)}(i'_{\ell,k}) + L_{\text{extr}}^{(C)}(i'_{\ell,k})$ for $\ell = 0, \ldots, M-1$, $k = 0, \ldots, N-1$. The term $L_c\,\hat{i}'_{\ell,k}$ is defined analog to (2) for the interleaved index bit $i'_{\ell,k}$. $L_a^{(C)}(i'_{\ell,k})$ denotes the *a priori* information for the index bit $i'_{\ell,k}$, and $L_{\text{extr}}^{(C)}(i'_{\ell,k})$ refers to the extrinsic information [13]. After subtraction of the *a priori* term and after deinterleaving we obtain the L-values $L_{\text{e}}^{(C)}(i_{\ell,k}) = L_c\,\hat{i}_{\ell,k} + L_{\text{extr}}^{(C)}(i_{\ell,k})$, which are used as *a priori* information $L_a^{(S)}(i_{\ell,k})$ for the SISO source decoder. In the following, we assume that all information bits are uncorrelated. Then, the corresponding index-based probabilities for the *a priori* L-values $L_a^{(S)}(i_{\ell,k})$ can be obtained by bitwise multiplication of the probabilities for the index bits $i_{\ell,k} = \lambda_\ell$. By inserting this *a priori* knowledge into (10) we obtain modified APPs according to

$$P'(I_k = \lambda \,|\, \hat{I}_k, \mathcal{N}_{\tilde{I}_k}) = C'_k \cdot P(I_k = \lambda \,|\, \mathcal{N}_{\tilde{I}_k}) \cdot \prod_{\ell=0}^{M-1} p(\hat{i}_{\ell,k} \mid i_{\ell,k} = \lambda_\ell)\, P_{\text{extr}}^{(C)}(i_{\ell,k} = \lambda_\ell \mid \hat{\boldsymbol{v}}) \qquad (13)$$

where C'_k is a normalizing constant (as above). Here, the iterative source decoding procedure described in Section 4 uses initial estimates $\tilde{I}_k^{(0)}$ obtained from the L-values $L^{(C)}(i'_{\ell,k})$ which belong to the channel-decoded information sequence $\pi(\boldsymbol{I})$. After the iterations have been performed, the output of the SISO source decoder corresponds to index-based modified APPs $P'(I_k = \lambda \,|\, \hat{I}_k, \mathcal{N}_{\hat{I}_k})$, where the related bit-based L-values can be derived for $\ell = 0, 1, \ldots, M-1$ as

$$L^{(S)}(i_{\ell,k}) = \ln \left(\frac{\sum_{\mu \in \mathcal{I}: \mu_\ell = 0} P'(I_k = \mu \,|\, \hat{I}_k, \mathcal{N}_{\hat{I}_k})}{\sum_{\mu \in \mathcal{I}: \mu_\ell = 1} P'(I_k = \mu \,|\, \hat{I}_k, \mathcal{N}_{\hat{I}_k})} \right). \qquad (14)$$

By subtracting the source *a priori* information $L_a^{(S)}(i_{\ell,k})$ from $L^{(S)}(i_{\ell,k})$ in (14) we finally obtain the extrinsic information $L_{\text{extr}}^{(S)}(i_{\ell,k})$, which is used as *a priori* information for subsequent channel decoding.

6 Simulation Results

An experimental image transmission system is now derived by applying the transmission model from Fig. 1 to every subband of an L-level wavelet octave filter bank and using the results from above.

The K 2-D subband signals are first scanned in a meander-type fashion [7] and quantized with optimal scalar quantizers. Then, the resulting bitstream in each subband is bit-interleaved using a random interleaver and channel encoded with a terminated memory-4 recursive systematic convolutional (RSC) code derived from a nonrecursive RCPC code [14]. In our setup we assume that sensitive side information, such as the lowpass subband DC content, quantizer stepsizes, and rate allocations, are protected by a sufficiently strong channel code, so that they can be transmitted without errors.

The experimental image transmission system is applied to the 512×512 pixel "Goldhill" test image for a 3-level wavelet decomposition and an overall target bit rate of $R_T = 0.37$ bits per pixel (bpp) including channel coding and all side information. This approach is denoted with "MRF JSCD" in the simulations. We have found experimentally that for the LL-subband only the horizontally and vertically oriented two-element cliques in Fig. 2 have to be considered, whereas for the rest of the subbands all possible two-element cliques are used. Note that in the presented MRF source model the number of pixels and their position within a local neighborhood mainly represent free variables (besides the temperature and the potential function) to obtain a suitable approximation of the probability distribution for the subband image indices. The further MRF parameters are $\delta = 0.7$, $T = 2.8$ for the LL subband, and $T = 4$ for all other subbands, respectively. Furthermore, we allow four iterations in the MRF source decoder. We compare the performance of the presented approach with the method from [7] ("2-D JSCD") which employs the same rate allocation strategy and a similar iterative source-channel decoding setup, but a different source model. In this model, horizontal and vertical correlations are regarded as separate Markov sources, where the transition probabilities corresponding to these Markov processes are obtained from a large training set and stored at the decoder. Besides, plain MRF-based source decoding ("MRF SD") [6] without additional protection by channel codes is also considered for comparison purposes. For all approaches, a mean-squares estimation is employed.

Fig. 4 shows the simulation results[1] for the above-mentioned methods where the peak-SNR (PSNR) values of the reconstructed images versus the channel parameter E_b/N_0 averaged over 100 simulated transmissions are displayed. We can see from Fig. 4 that especially for low channel SNR the "MRF JSCD" technique outperforms the "2-D JSCD" approach by approximately 1-2 dB in PSNR. This performance gain may be due to the fact that the MRF source decoding itself is performed iteratively, such that the channel decoder can be provided with more reliable L-values for the next iteration between source and channel decoder. For channels with an $E_b/N_0 > 1$ dB both approaches have approximately the same performance. In our simulations we observed that the "MRF JSCD" approach approximately has the same complexity as the "2-D JSCD" approach. However, the storage complexity is significantly reduced for the proposed MRF-based JSCD approach since there is no need to store source *a priori* information. By comparison with the results for the "MRF SD" approach we can see that we gain up to almost 3 dB in PSNR for the *same* target rate R_T by adding explicit redundancy from channel codes in combination with a joint rate allocation at the encoder and an iterative source-channel decoder. An example of the good reconstruction quality for a highly corrupted channel is displayed in Fig. 5.

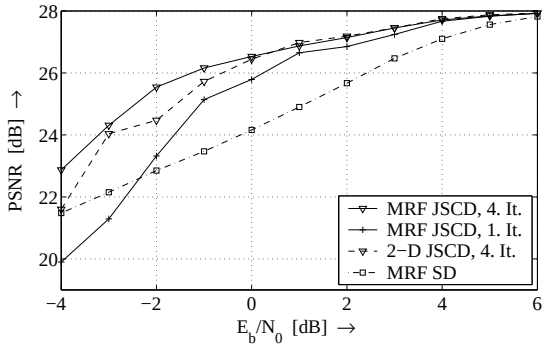

Fig. 4. Results for the "Goldhill" image ($R_T = 0.37$ bpp, $L = 3$)

Fig. 5. Reconstructed "Goldhill" image for $E_b/N_0 = -1$ dB (BER 10.4 %), PSNR: 26.23 dB ($R_T = 0.37$ bpp, $L = 3$, MRF JSCD, four iterations).

The simulation results for the "Lena" test image are shown in Fig. 6, where the same simulation parameters as for the "Goldhill" image are used. We can see that here for $E_b/N_0 > 0$ dB the "MRF JSCD" approach is

[1] Since the rate allocation algorithm only searches for operation points on the convex hull in the rate-distortion plane [10], for some values of E_b/N_0 we obtain an overall bit rate being slightly smaller than the target rate R_T. Thus, the curves for the JSCD techniques in both Fig. 4 and Fig. 6 lack the smooth behavior of those for the pure MRF source decoding approach.

even able to give slightly better results than the "2-D JSCD" technique.

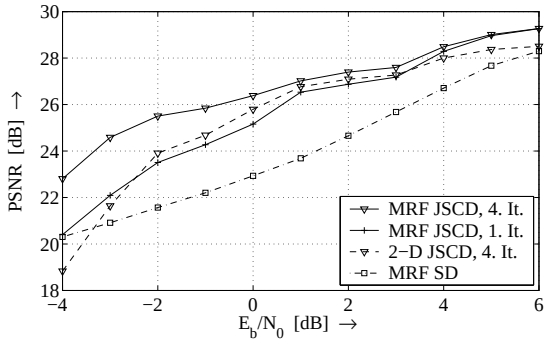

Fig. 6. Results for the "Lena" image ($R_T = 0.37$ bpp, $L = 3$)

Besides plotting the SNR-PSNR performance the iterative MRF-based source-channel decoder can also be analyzed via EXIT charts [15] which show the input-output characteristics of the constituent decoders in terms of mutual information $I(\cdot\,;\cdot)$ between L-values and the index sequence $\boldsymbol{I}$. Given the mutual informations (cmp. Fig. 3)

$$I_{E_i} := I(L_e^{(C)}(\pi(\boldsymbol{I}));\pi(\boldsymbol{I})), \quad I_{A_i} := I(L_a^{(C)}(\pi(\boldsymbol{I}));\pi(\boldsymbol{I})),$$
$$I_{E_o} := I(L_{\text{extr}}^{(S)}(\boldsymbol{I});\boldsymbol{I}), \qquad I_{A_o} := I(L_a^{(S)}(\boldsymbol{I});\boldsymbol{I}),$$

the transfer characteristics T_i of the (inner) channel decoder and T_o of the (outer) MRF SISO decoder are defined as $I_{E_i} = T_i(I_{A_i}, E_b/N_0)$ and $I_{E_o} = T_o(I_{A_o})$, respectively. By plotting both mappings T_i and T_o into one diagram we obtain an EXIT chart, where an example for the LL subband of the "Goldhill" image and an $E_b/N_0 = -1$ dB is depicted in Fig. 7. In order to illustrate the iterative decoding process Fig. 7 also displays snapshot decoding trajectories, where we can observe that after two iterations convergence is already obtained.

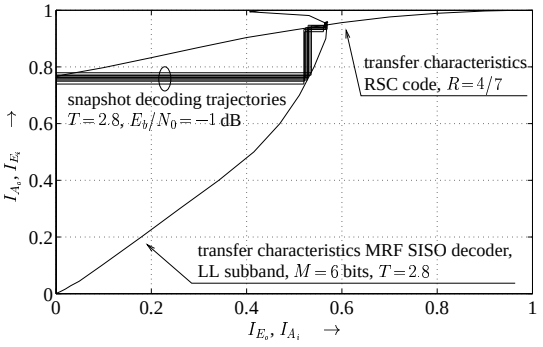

Fig. 7. EXIT chart for the LL subband of the "Goldhill" image and $E_b/N_0 = -1$ dB

7 Conclusions

By using the implicit two-dimensional residual source redundancy for error protection in conjunction with channel coding, an iterative decoding scheme is derived in a similar way as for serially concatenated channel codes: the difference is that a soft-input APP source decoder replaces the outer constituent channel decoder. The source signals are modeled using Markov random fields, and due to the Markov-Gibbs correspondence, the computation of *a priori* densities can be made very resource-efficient. We have shown that this source-channel decoding technique, in combination with a novel joint source-channel rate-allocation, can be used for robust image transmission over highly distorted AWGN channels. The advantage of the proposed method is that by incorporating residual redundancies into the decoding process, less powerful channel codes can be chosen, which also reduce the complexity of the encoder and the encoding delay. The simulation results show that the clear-channel quality is already achieved for moderately distorted channels.

References

[1] P. G. Sherwood and K. Zeger, "Error protection for progressive image transmission over memoryless and fading channels," *IEEE Trans. on Comm.*, vol. 46, no. 12, pp. 1555–1559, 1998.

[2] V. Chande and N. Farvardin, "Joint source-channel coding for progressive transmission of embedded source coders," in *Proc. IEEE Data Compression Conference*, Snowbird, UT, USA, Mar. 1999, pp. 52–61.

[3] H. H. Otu and K. Sayood, "A joint source/channel coder with block constraints," *IEEE Trans. on Comm.*, vol. 47, no. 22, pp. 1615–1618, Nov. 1999.

[4] M. Park and D. J. Miller, "Improved image decoding over noisy channels using minimum mean-squared estimation and a Markov mesh," *IEEE Trans. on Image Proc.*, vol. 8, no. 6, pp. 863–867, June 1999.

[5] S. Geman and D. Geman, "Stochastic relaxation, Gibbs distribution, and the Bayesian restoration of images," *IEEE Trans. on Pattern Analysis and Machine Intelligence*, vol. PAMI-6, no. 6, pp. 721–741, Nov. 1984.

[6] A. Mertins, "Image recovery from noisy transmission using soft bits and Markov random fi eld models," *Optical Engineering*, vol. 42, no. 10, pp. 2893–2899, Oct. 2003.

[7] J. Kliewer and N. Goertz, "Iterative source-channel decoding for robust image transmission," in *Proc. IEEE Int. Conf. Acoust., Speech, Signal Processing*, Orlando, FL, USA, May 2002, pp. 2173–2176.

[8] N. Goertz, "On the iterative approximation of optimal joint source-channel decoding," *IEEE Journal on Sel. Areas in Comm.*, vol. 14, no. 9, pp. 1662–1670, Sept. 2001.

[9] S. Benedetto, D. Divsalar, G. Montorsi, and F. Pollara, "Serial concatenation of interleaved codes: Performance analysis, design, and iterative decoding," *IEEE Trans. on Inf. Theory*, vol. 44, no. 3, pp. 909–926, May 1998.

[10] Y. Shoham and A. Gersho, "Effi cient bit allocation for an arbitrary set of quantizers," *IEEE Trans. on Acoust., Speech, Signal Processing*, vol. 36, no. 9, pp. 1445–1453, Sept. 1988.

[11] T. M. Cover and J. A. Thomas, *Elements of Information Theory*, Wiley, New York, 1991.

[12] C. A. Bouman and K. Sauer, "A generalized Gaussian image model for edge-preserving MAP estimation," *IEEE Trans. on Image Processing*, vol. 2, no. 3, pp. 296–310, July 1993.

[13] J. Hagenauer, E. Offer, and L. Papke, "Iterative decoding of binary block and convolutional codes," *IEEE Trans. on Inf. Theory*, vol. 42, no. 2, pp. 429–445, Mar. 1996.

[14] J. Hagenauer, "Rate-compatible punctured convolutional codes (RCPC codes) and their appplications," *IEEE Trans. on Comm.*, vol. 36, no. 4, pp. 389–400, Apr. 1988.

[15] S. ten Brink, "Code characteristic matching for iterative decoding of serially concatenated codes," *Annals of Telecomm.*, vol. 56, no. 7-8, pp. 394–408, July-August 2001.